

## Cotton-Mouton polarimeter with HCN laser on CHS

T. Akiyama, K. Kawahata, and Y. Ito

*National Institute for Fusion Science, 322-6 Oroshi-cho, Toki-shi, Gifu 509-5292, Japan*

S. Okajima and K. Nakayama

*Chubu University, Matsumoto-cho, Kasugai-shi, Aichi 487-8501, Japan*

S. Okamura, K. Matsuoka, M. Isobe, S. Nishimura, C. Suzuki, Y. Yoshimura, K. Nagaoka, C. Takahashi, and CHS Experimental Group

*National Institute for Fusion Science, 322-6 Oroshi-cho, Toki-shi, Gifu 509-5292, Japan*

(Received 6 May 2006; presented on 10 May 2006; accepted 26 June 2006; published online 6 October 2006)

Polarimeters based on the Cotton-Mouton effect hold promise for electron density measurements. We have designed and installed a Cotton-Mouton polarimeter on the Compact Helical System. The Cotton-Mouton effect is measured as the phase difference between probe and reference beams. In this system, an interferometric measurement can be performed simultaneously with the same probe chord. The light source is a HCN laser (wavelength of 337  $\mu\text{m}$ ). Digital complex demodulation is adopted for small phase analysis. The line averaged density evaluated from the polarimeter along a plasma center chord is almost consistent with that from the interferometer. © 2006 American Institute of Physics. [DOI: 10.1063/1.2229275]

### I. INTRODUCTION

A polarimeter for electron density measurements in magnetically confined plasmas is expected to be robust even in a high-density range. The reasons are as follows. It is free from fringe jump errors and is immune to the effects of mechanical vibrations, which degrade the reliability and resolution of an interferometer.

There are two types of polarimeters, based on the Faraday and on the Cotton-Mouton effect, respectively. These two magneto-optic effects depend, respectively, on the magnetic fields parallel and perpendicular to the propagation direction of an electromagnetic wave in a plasma. Therefore, one of them is chosen according to the beam path. In the case of the electron density measurement in a plasma center chord in a poloidal cross section, only the Cotton-Mouton polarimeter is available; the Faraday effect is too small, due to the absence of a magnetic field component parallel to the beam path. On the other hand, polarimeters based on the Faraday effect are usually applied for tangential measurement.<sup>1-3</sup>

Although a Cotton-Mouton polarimeter has recently been developed<sup>4-6</sup> and is proposed for the International Thermonuclear Experiment Reactor (ITER),<sup>7</sup> its applications are fewer than those of Faraday polarimeters. We have developed a Cotton-Mouton polarimeter using a HCN laser (wavelength of 337  $\mu\text{m}$ ) on the Compact Helical System (CHS).<sup>8</sup> The method of measuring the Cotton-Mouton effect as a phase difference is adopted. It is insensitive to amplitude variations of detected signals due to oscillation instabilities of the laser and beam refraction in the plasma. Here, in order to assess the accuracy and measurement errors of the Cotton-Mouton polarimeter, it is combined with an interferometer that can operate simultaneously using the same probe beam.

### II. SYSTEM DESIGN

#### A. Theoretical and numerical estimation

For the description of the polarization state and evolution in magnetized plasmas, Stokes vector  $\mathbf{s}$  and plasma Mueller matrix  $\mathbf{M}$  are introduced here.<sup>9</sup> The following differential equation describes the evolution of the polarization state (electromagnetic wave propagates along the  $z$  direction):

$$\frac{d\mathbf{s}(z)}{dz} = \mathbf{\Omega}(z) \times \mathbf{s}(z), \quad (1)$$

where

$$\mathbf{\Omega} = \begin{pmatrix} \Omega_1 \\ \Omega_2 \\ \Omega_3 \end{pmatrix} = \frac{1}{16\pi^3 c^4} \left( \frac{n_c e^2}{\varepsilon_0 m_e} \right) \lambda^3 \begin{bmatrix} \left( \frac{e}{m_e} \right)^2 (B_y^2 - B_x^2) \\ 2 \left( \frac{e}{m_e} \right)^2 B_y B_x \\ \frac{4\pi c}{\lambda} \left( \frac{e}{m_e} \right) B_z \end{bmatrix} \quad (2)$$

and  $\varepsilon_0$  is the permittivity,  $c$  is the light speed,  $\lambda$  is the wavelength of the electromagnetic wave,  $m_e$  and  $e$  are the mass and the charge of an electron, and  $B_x$ ,  $B_y$ , and  $B_z$  are components of the magnetic field. The Cotton-Mouton effect corresponds to the first and the second components and the Faraday effect the third. Putting  $\mathbf{s}$  in the form

$$\mathbf{s}(z_1) = \mathbf{M}(z_1) \mathbf{s}(z_0) \quad (3)$$

and considering the symmetry of the magnetic field along the vertical propagation (the  $z$  direction) in a poloidal cross section (the  $y$  direction corresponds to the toroidal direction), we obtain

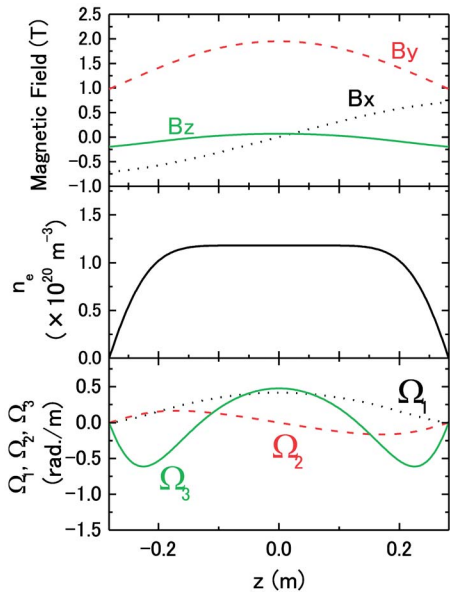


FIG. 1. (Color online) Distributions of the magnetic field components, a typical electron density profile, and components of  $\Omega$  along a plasma center chord in a CHS plasma ( $R_{ax}=92.1$  cm and  $B_{ax}=1.96$  T).  $\Omega$  is the calculation results in the case of the wavelength of the HCN laser.

$$M(z_1) \approx \begin{bmatrix} 1 & -(W_3 - W_{21}) & W_1 W_3 / 2 \\ (W_3 - W_{21}) & 1 & -(W_1 - W_{32}) \\ W_1 W_3 / 2 & (W_1 - W_{32}) & 1 \end{bmatrix}, \quad (4)$$

where

$$W_j = \int_{z_0}^{z_1} dz \Omega_j(z), \quad W_{jk} = \int_{z_0}^{z_1} dz \Omega_j(z) \int_{z_0}^z dz' \Omega_k(z').$$

Note that this is the approximate solution of  $M$  when  $W_1^2 \ll 1$ ,  $W_3^2 \ll 1$  ( $W_2=0$  from up/down symmetry), namely, when the Faraday and Cotton-Mouton effects are small.

For the phase measurement of the Cotton-Mouton effect, probe and reference beams whose polarization states are modulated with a frequency of  $\omega_b$  (Ref. 9) are used. As shown in the next section, the beam consists of orthogonally and linearly polarized beams with a frequency difference of  $\omega_b$ . The Stokes vector of such a beam is  $s(z_0) = (0, \cos \omega_b t, \sin \omega_b t)$ . Using Eq. (4) for  $M$ , the second component of  $s(z_1)$ , which shows a polarization state after passing through a plasma (probe beam), becomes  $s_2 = \cos \omega_b t$

$-(W_1 - W_{32}) \sin \omega_b t$ . By setting a polarizer with the transmission angle  $\pi/4$  at the  $x$  direction in front of a detector, the following detected signal  $I$  is obtained:

$$2II_0 = 1 + s_2 = 1 + \cos \omega_b t - (W_1 - W_{32}) \sin \omega_b t \approx 1 + C \cos[\omega_b t + \tan^{-1}(W_1 - W_{32})],$$

where  $I_0$  is the intensity of the entering beam and  $C$  is a constant.

In addition to the Cotton-Mouton effect  $W_1$ , the phase of the detected signal contains an error term  $W_{32}$  for the density evaluation. Figure 1 shows the distributions of the magnetic field components in the vacuum configuration, the typical electron density profile, and  $\Omega$  for a wavelength of  $337 \mu\text{m}$  along the plasma center chord in the CHS plasma. In this calculation the position of the magnetic axis  $R_{ax}$  is set at the major radius of 92.1 cm, and the magnetic field strength at the magnetic axis  $B_{ax}$  is 1.96 T. A flat density profile is typical in a neutral beam (NB) heated plasma in CHS. Therefore, the electron density profile is assumed to be  $1.2 \times 10^{20} (1 - \rho^8) \text{ m}^{-3}$ , with a line averaged electron density  $\bar{n}_e$  of  $1 \times 10^{20} \text{ m}^{-3}$  in the plasma center chord. Here,  $\rho$  is the normalized magnetic flux radius. In this condition,  $W_1 = 8.2^\circ$ ,  $W_2 = 0^\circ$ ,  $W_3 = 1.8^\circ$ , and  $W_{32} = 0.09^\circ$ .  $W_{32}$  is only 1% of  $W_1$  and is negligibly small although the  $B_x$  component is not small due to the strong magnetic shear in CHS. Thus the Cotton-Mouton effect can be estimated from the phase difference between the probe and the reference signals.

The  $B_y$  component cannot be regarded constant along the optical path shown in Fig. 1. Therefore, the line averaged electron density evaluated from the polarimeter  $\bar{n}_e^{CM}$  is weighted by the magnetic field, and the electron density in the plasma center region is emphasized. In this article, assuming the flat density profile and the magnetic field mentioned above,  $\bar{n}_e^{CM} (\times 10^{20} \text{ m}^{-3})$  is defined to be

$$\bar{n}_e^{CM} = W_1 / W_1 [n_e = 1.2 \times 10^{20} (1 - \rho^8) \text{ m}^{-3}] = W_1 / 8.2.$$

For example, in the case of a peaked density profile of  $1.6 \times 10^{20} (1 - \rho^2) \text{ m}^{-3}$ , whose  $\bar{n}_e$  is also  $1 \times 10^{20} \text{ m}^{-3}$ ,  $W_1$  is  $8.9^\circ$  and  $\bar{n}_e^{CM}$  is 8% larger than  $\bar{n}_e$ . Although  $\bar{n}_e^{CM}$  becomes slightly different from  $\bar{n}_e$  accordingly, as the density profile changes, it is supposed that  $\bar{n}_e^{CM}$  is sensitive to the behavior of the central electron density.

### B. Optical setup

Figure 2 shows the schematic illustration of the optical arrangement on CHS. This is the combined system of the

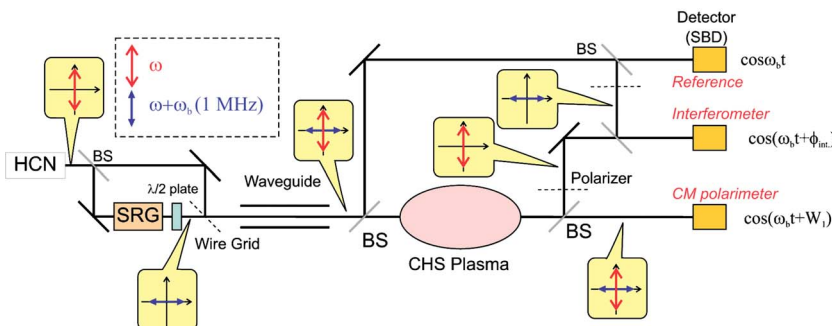


FIG. 2. (Color online) Schematic illustration of the optical arrangement of the Cotton-Mouton polarimeter combined with the interferometer on CHS.

Cotton-Mouton polarimeter and the interferometer. The basic idea of the combination is almost the same as that of the polarimeter proposed on W7-X.<sup>10</sup> The light source is the discharge-excited HCN laser,<sup>11</sup> whose operational output is about 100 mW (maximum of about 500 mW). Though a slightly longer wavelength is preferable for a good signal-to-noise ratio in the polarimeter ( $W_1$  is proportional to  $\lambda^3$ ), a HCN laser is selected for the suppression of the beam refraction, which leads to fringe jump errors in the interferometer. Instead, complex demodulation combined with digital filtering<sup>2,12</sup> is adopted to improve the phase resolution.

The HCN laser beam is split into two beams with a Mylar beam splitter and the frequency of one is shifted with a super rotation grating.<sup>13</sup> The frequency shift  $\omega_b$  is 1 MHz due to the high rotation speed (500 rps) of the rotating grating fabricated on the top of the magnetically floating rotor in the turbo molecular pump. After rotating the plane of polarization by  $\pi/2$ , two laser beams are combined with a wire grid (diameter and spacing of wires are 5 and 12.5  $\mu\text{m}$ , respectively, Graseby Specac Ltd.). In this way an elliptically modulated beam is generated. The laser beam is transmitted with waveguides (inner diameter of 47 mm) made of acrylic resin to CHS. The total transmission efficiency is about 80% (path length is about 15 m). The beam is split into probe and reference beams with a crystal quartz beam splitter, and they are injected into the vacuum vessel through a crystal quartz window. They are detected with Schottky barrier diodes (SBDs, Farran Technology). Since only the polarization component parallel to a receiving antenna in the SBD is detected, SBDs are tilted by  $\pi/4$ , and they obviate polarizers. After passing through an analog bandpass filter and an amplifier, 1 MHz beat signals of the polarimeter's probe and reference are digitized at a frequency of 5 MHz. Then, complex demodulation is applied and the phase difference is extracted. For the interferometric measurement, the probe beam is split after passing through the plasma, and one polarization component (the  $O$  mode) is selected with a polarizer. The transverse polarization component is selected from the reference beam and then they are combined. The 1 MHz beat signal is obtained in the same way. The phase shift of the signal  $\phi_{\text{int}}$  corresponds to the phase shift of the  $O$ -mode component in the plasma. The phase shift is detected with a phase counter made at the National Institute for Fusion Science (NIFS).<sup>14</sup>

### III. EXPERIMENTAL RESULTS

As pointed out in Refs. 5 and 15, multireflection between the detector and optical components (called "back-talk") causes spurious oscillations in the phase difference of the polarimeter. In addition, electrical cross-talk between beat signals of the polarimeter and the interferometer also causes oscillations. The backtalk was reduced by inserting an attenuation in front of the SBD because the multireflection passed through it several times and became small. The electrical cross-talk was improved by changing the electrical circuit in the bandpass filter. Figure 3 shows the standard deviation of the phase difference as a function of the response time that is determined by the bandwidth of the digital bandpass filter. For example, the standard deviations are about

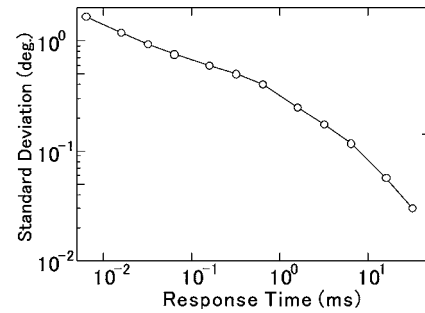


FIG. 3. Standard deviation of phase difference as a function of response time, determined by the bandwidth of the digital bandpass filter.

$0.50^\circ$  and  $0.17^\circ$  (corresponding to  $\Delta\bar{n}_e$  of  $6.1 \times 10^{18}$  and  $2.1 \times 10^{18} \text{ m}^{-3}$ ) with response times of 0.32 and 3.2 ms, respectively. The noises in the phase difference signal are attributed to the frequency noises of the 1 MHz beat signal. The frequency of the beat signal is slightly modulated with a period equal to the rotation period of the grating of the SRG. That is caused by the misalignment between the rotor axis and the grating.<sup>12</sup> To improve the resolution, it is necessary to replace the grating or to adopt a twin laser system.

Figure 4 shows measurement results of the polarimeter and the interferometer along the plasma center chord. The combined interferometer works successfully and  $\bar{n}_e$  agrees with that measured with the existing 2 mm wave interferometer (not shown). The result of the polarimeter is almost consistent with that of the interferometer. The response time of the polarimeter in Fig. 4 is 0.32 ms. However, there are still slight differences between them. Possible reasons include changes in the magnetic field due to a finite  $\beta$  effect, changes in the electron density profile, and residual cross- and back-talk components. In particular,  $\bar{n}_e^{\text{CM}}$  remains at zero in the low but finite density range. Since  $\bar{n}_e^{\text{CM}}$  in the low-density range sometimes seems to go negative, the first and the second speculations cannot explain the discrepancy in the low-density range. Though the third might seem the most possible at present, the frequencies of the residual oscillation are rather small (about one-quarter) compared to those removed. Therefore, the explanation based on cross- and backtalk remains in question.

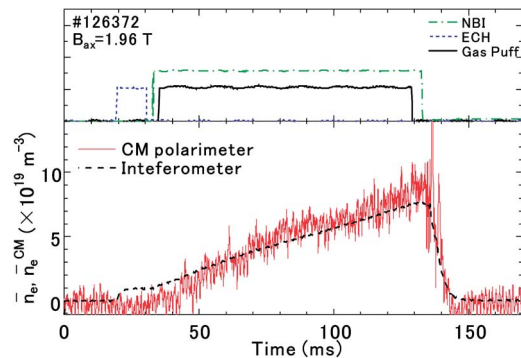


FIG. 4. (Color online) Line averaged densities evaluated from the interferometer and the Cotton-Mouton polarimeter. The response time is 0.32 ms.

#### IV. SUMMARY

We developed a Cotton-Mouton polarimeter with a HCN laser on CHS. This system is combined with an interferometer. The ellipticity of probe and reference beams is modulated to measure the Cotton-Mouton effect as a phase difference. The present standard deviation of density derived from the polarimeter is  $6.1 \times 10^{18} \text{ m}^{-3}$  with a response time of 0.32 ms; the noises are mainly caused by beat frequency noises. Measurement results of the polarimeter in a plasma center chord show good agreement with those of the interferometer.

#### ACKNOWLEDGMENTS

This work is supported by funds of NIFS05 ULPD603 and the Grant-in-Aid for Scientific Research on Priority Area "Advanced Diagnostics for Burning Plasmas" (16082208). The authors thank the Inoue Foundation for Science for supporting the presentation of this article.

- <sup>1</sup>Y. Kawano, S. Chiba, and A. Ioué, *Rev. Sci. Instrum.* **72**, 1068 (2001).
- <sup>2</sup>T. Akiyama *et al.*, *Rev. Sci. Instrum.* **74**, 2695 (2003).
- <sup>3</sup>H. K. Park, C. W. Domier, W. R. Geck, and N. C. Luhmann, Jr., *Rev. Sci. Instrum.* **70**, 710 (1999).
- <sup>4</sup>V. F. Shevchenko, A. A. Petrov, V. G. Petrov, and Y. A. Chaplygin, *Plasma Phys. Rep.* **22**, 28 (1996).
- <sup>5</sup>Ch. Fuchs and H. J. Hartfuss, *Phys. Rev. Lett.* **81**, 1626 (1998).
- <sup>6</sup>K. Guenther and JET EFDA Contributors, JET EFDA Paper No. EFDA-JET-CP(04)03-21 (unpublished).
- <sup>7</sup>A. J. H. Donne *et al.*, *Rev. Sci. Instrum.* **75**, 4694 (2004).
- <sup>8</sup>S. Okamura *et al.*, *Nucl. Fusion* **39**, 1337 (1999).
- <sup>9</sup>S. E. Segre, *Plasma Phys. Controlled Fusion* **41**, R57 (1999).
- <sup>10</sup>Ch. Fuchs, Diagnostics Proposal on Cotton-Mouton Polarimeter (sub-mm/IR) for W7-X, 9/2000.
- <sup>11</sup>S. Okajima, K. Kawahata, T. Tetsuka, S. Kubo, and J. Fujita, *Digest of the 11th International Conference on IR and MM Waves, Pisa, 1986*, p. 249.
- <sup>12</sup>Y. Jiang, D. L. Brower, L. Zeng, and J. Howard, *Rev. Sci. Instrum.* **68**, 902 (1997).
- <sup>13</sup>T. Maekawa, T. Minami, K. Makino, S. Tanaka, S. Kubo, and M. Iguchi, *Rev. Sci. Instrum.* **62**, 304 (1991).
- <sup>14</sup>Y. Ito, K. Haba, T. Tokuzawa, and K. Kawahata, *Fusion Eng. Des.* **56-57**, 965 (2001).
- <sup>15</sup>D. Elbèze, C. Gil, R. Gianella, L. De Pasqual, and JET-EFDA Contributors, *Rev. Sci. Instrum.* **75**, 3405 (2004).